IEEE Transactions on Nuclear Science, Vol.NS-22, No.3, June 1975

COMPRESSION OF ELECTRON RING: THE SYSTEM AND RESULTS IN IPP-JAPAN

S. Kawasaki,* N. Kobayashi, Y. Kubota and A. Miyahara
Institute of Plasma Physics, Nagoya University, 464 Nagoya, Japan

Summary

The exact solution of the magnetic field produced by the pulsive current flowing in the coils placed inside the metal vacuum chamber of ERA device in IPP-Nagoya, is calculated to design the compression system of the electron ring. Actual design of the compression coils and installations of power supply systems are also described.

Introduction

In ERA of IPP-Nagoya, the vacuum chamber has a relatively simple form and the pill-box model could be well applied to calculate the instabilities and the beam-wall interaction which are anticipated to appear. It is made of stainless steel walls of 0.6-1.5 cm thick, and keeps a good vacuum better than 10^{-8} torr (Fig.1).

The fact that the coil for compression should be placed inside the metal wall causes some technical problems in construction of the coils: the feeding of high power through the wall, high voltage insulation inside the high vacuum etc. Moreover, the frequency of the exciting current is sufficiently high so that the pulsive magnetic field can not penetrate into the metal walls, or the magnetic field produced by the induced current on the surface wall should be added to the field by the primary current flowing in the coils.

In this work, the magnetic field and the inductance of the coils are calculated exactly taking into account the effect of the metal walls, with a simplified model of the wall geometry, and the design of the power supply is given.

Magnetic Field in the Conductive Boundaries

We neglect the effect of the holes for the electric feeders and the evacuation, as well as the existence of the inflector plates near the electron beam, while they are also conductive. The conductivity of the wall is supposed to be infinitive. The magnetic field determined by the currents flowing in the coils, the position of which is shown in Fig.2, is calculated exactly with the framework of the classical electrodynamics. Several pairs of coils are placed symmetrically with the median plane of the chamber. The field with the single pair of one-turn coils shown in the figure, can be composed of giving the field distributions for any given geometry of coils. The required boundary conditions are

$$B_r = 0 \quad \text{at} \quad r = b \quad \text{and for} \quad -h \leq z \leq h$$
$$B_z = 0 \quad \text{at} \quad z = \pm h \quad \text{and for} \quad 0 \leq r \leq b \qquad 1)$$

where the cylindrical co-ordinates and MKS units are used. The second of the equations 1) is automatically satisfied, supposing the infinite series of the image current as shown in Fig.3. The current density $\vec{j}$ is given by

$$j = j_0[\delta(z \pm s + 4mh) + \delta(z \mp 2h \pm s + 4nh)] \qquad 2)$$

where m and n are arbitrary integers.

If the displacement current can be neglected, in this case the basic equations only one of the Maxwell's equations,

$$\text{rot}\,\vec{B} = \mu\vec{j} \qquad 3)$$

with the axial symmetric configuration of the system, the non-vanishing component of $\vec{A}$ is A_ϕ and its azymuthal dependence disappears. The resulted expressions for the vector potentials inside and outside the radius of the coil, A_ϕ and A'_ϕ

$$A_\phi = \frac{\mu ai}{2h}\sum_{m=1}^{\infty} I_1(\frac{\pi ma}{2h})[K_1(\frac{\pi mr}{2h}) - K_1(\frac{\pi mb}{2h})\frac{I_1(\frac{\pi mr}{2h})}{I_1(\frac{\pi mb}{2h})}]$$
$$[\cos(\frac{\pi m(z+s)}{2h}) + \cos(\frac{\pi m(z-s)}{2h}) - \cos(\frac{\pi m(z-2h+s)}{2h}) - \cos(\frac{\pi m(z+2h-s)}{2h})] \quad \text{for} \quad a \leq r \leq b \qquad 4)$$

and

$$A'_\phi = \frac{\mu ai}{2h}\sum_{m=1}^{\infty} I_1(\frac{\pi mr}{2h})[K_1(\frac{\pi ma}{2h}) - K_1(\frac{\pi mb}{2h})\frac{I_1(\frac{\pi ma}{2h})}{I_1(\frac{\pi mb}{2h})}]$$
$$[\cos(\frac{\pi m(z+s)}{2h}) + \cos(\frac{\pi m(z-s)}{2h}) - \cos(\frac{\pi m(z-2h+s)}{2h}) - \cos(\frac{\pi m(z+2h-s)}{2h})] \quad \text{for} \quad r \leq a \qquad 5)$$

It should be noted that the homogeneous component for m = 0 disappears. For the analysis of the beam dynamics, the magnetic field on the median plane z = 0 is of primary importance. The term in the second parenthesis in 4) and 5) is $-4\sin\pi m/2\sin\pi m(s-h)/4$ for z = 0. Now we assume the coil position in the axial direction, as s = h/2. The magnetic field on the median plane, $H_z(z=0)$ is

$$H_z(z=0) = \frac{2ai}{h}\sum_{m=1}^{\infty} I_1(\frac{\pi ma}{2h})[-K_0(\frac{\pi mr}{2h})\frac{m\pi}{2h} - \frac{K_1(\frac{\pi mb}{2h})}{I_1(\frac{\pi mb}{2h})} \times I_0(\frac{\pi mr}{2h})\frac{m\pi}{2h}]\sin\frac{\pi m}{2}\sin\frac{\pi m}{4} \quad \text{for} \quad a \leq r \leq b \qquad 6)$$

and

$$H_z(z=0) = \frac{2ai}{h}\sum_{m=1}^{\infty} I_0(\frac{\pi mr}{2h})\frac{m\pi}{2h}[K_1(\frac{\pi ma}{2h}) - K_1(\frac{\pi mb}{2h})\frac{I_1(\frac{\pi ma}{2h})}{I_1(\frac{\pi mb}{2h})}] \times \sin\frac{\pi m}{2}\sin\frac{\pi m}{4} \quad \text{for} \quad r \leq a \qquad 7)$$

The magnetic field H_z calculated by 6) and 7) are easily shown to take the same value at r = a.

With the parameters of the experimental system in IPP-Nagoya, h = 12 cm b = 30 cm and s = 6 cm, for various values of a, 6) and 7) are calculated numerically to give the magnetic field on the median plane as shown in Fig.4(A)-(H).

Coil Inductance

To find the coil inductance of the coil pair placed at r = a, the magnetic flux Φ linked up with the coil is calculated:

$$\Phi = \frac{\pi\mu ai}{h}(a-d)\sum_{m=1}^{\infty} I_1[\frac{\pi m}{2h}(a-d)][K_1(\frac{\pi ma}{2h}) - K_1(\frac{\pi mb}{2h}) \times \frac{I_1(\frac{\pi ma}{2h})}{I_1(\frac{\pi mb}{2h})}][\cos\frac{\pi ms}{h}\cos\frac{\pi m(s-h)}{h} - \cos\frac{\pi m(s+h)}{h}] \qquad 8)$$

The inductance of the coil pair in parallel is $L = \frac{\Phi}{2i}$. If we connect the coil pair in series the inductance

* Faculty of Science, Kanazawa University, 920 Kanazawa, Japan.

is 4 times larger. The flux Φ for a unit flowing current i is calculated numerically and shown in Fig.5 as a function of the coil position a, where the radial halfwidth is supposed to be 0.5 cm. The self inductance of the coil $L_{self} = \mu a(\ell n(8a/d)-2)$ should be added to 8) to obtain the total inductance.

Actual Design of the Compression Coils

In the ERA experiment of IPP-Nagoya, the first aim is to investigate the beam behavior in the early period of the ring formation and the beam-wall interaction with various parameters of the injected electrons. The later stage of the compression seems to have little difficulty. From this point of view only two coils are prepared to compress the ring radially by a factor of about 2. Positions of the coils determined by the above analysis, are shown in Fig.1. Their geometrical and electrical parameters are listed in Table I. The feeding of the exciting current into the coils are through the connections of ceramic feedthrough. Insulations of the high voltage and reduction of the stray inductance were the objects of our hard considerations. Block diagram of compression coil system, power supply system and triggering system is given in Fig.6. This system has just completed and start to operate with the injected beams of 2 MeV 1 kA. Investigations about compression dynamics are under going.

Acknowledgments

The authors express their sincere thanks to Mr. J. Kodaira, who carried out numerical computations of this paper.

Table I. Parameters of compression coil system.

	Coil 1	Coil 2
Inner Radius	240 mm	170 mm
Outer Radius	280 mm	190 mm
Axial Width	5 mm	10 mm
Total Inductance	0.5 μH	0.45 μH
Max. Current	11.4 kA	69 kA
Capacitor	0.15 μF	2.97 μF
Charging Voltage	20 kV	20 kV

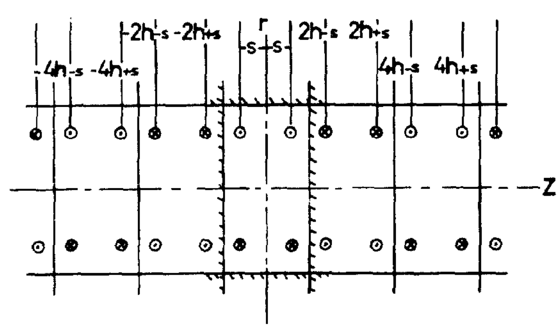

Fig.3. The arrangements of the image currents to satisfy the second of the required boundary conditions.

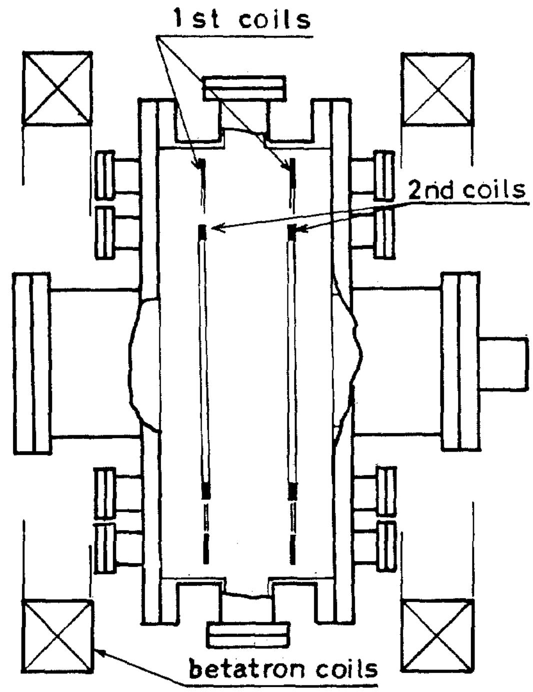

Fig.1. The vacuum chamber of ERA devide in IPP-Nagoya.

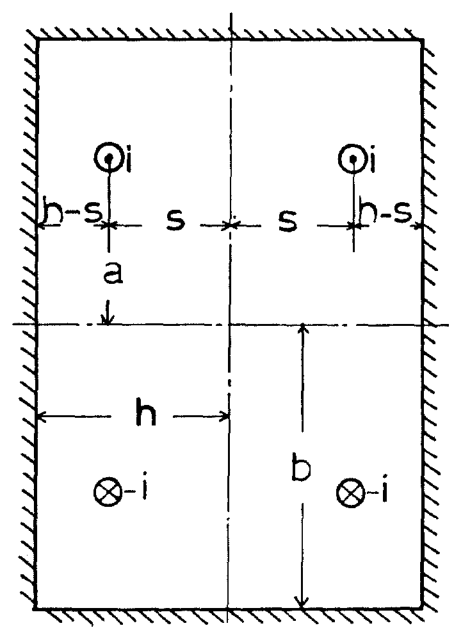

Fig.2. The pair coil position in a pill-box like conductive boundaries.

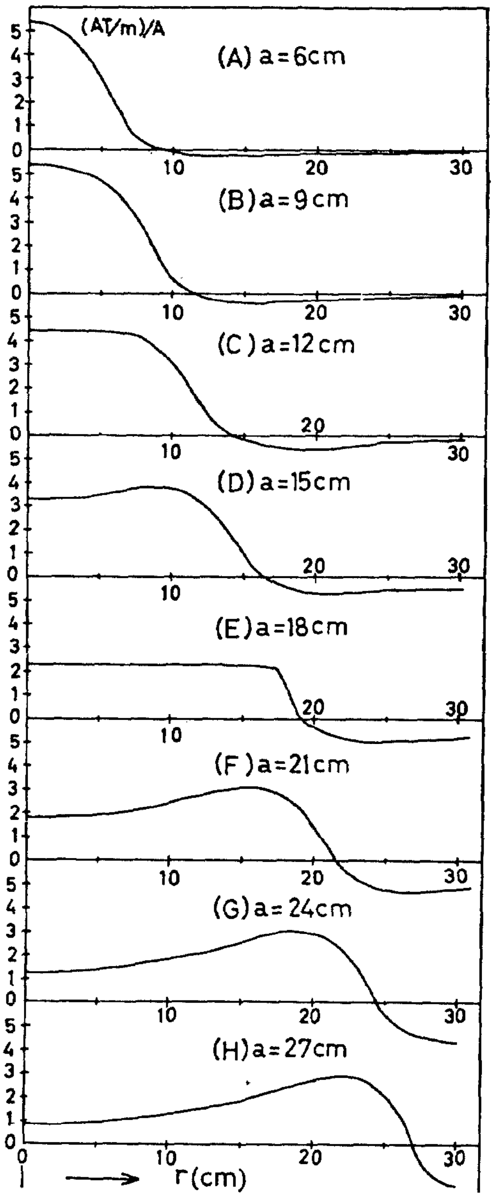

Fig.4(A)-(H). The magnetic field on the median plane for various values of the coil position in the radial direction, a.

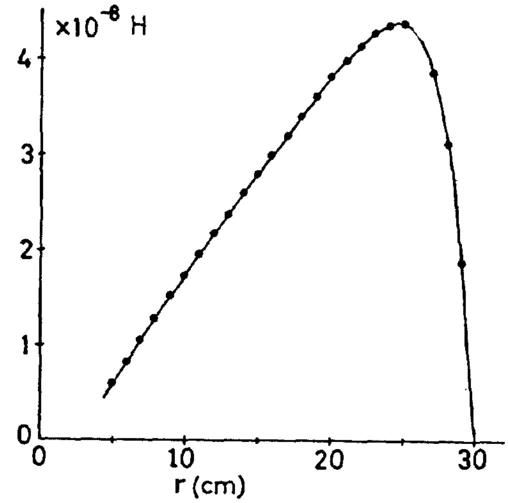

Fig.5. The inductance of the coil pair shown in Fig.2 for various values of a.

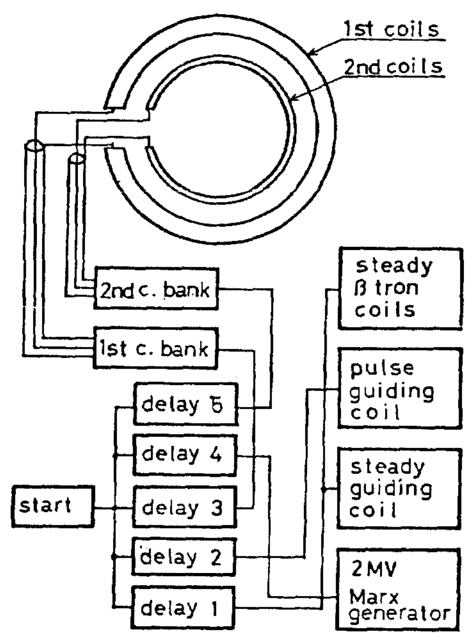

Fig.6. The block diagram of ERA device.